ADVANCES IN ATMOSPHERIC SCIENCES, VOL. 35, SEPTEMBER 2018, 1145–1159

• **Original Paper** •

Source Contributions to $PM_{2.5}$ under Unfavorable Weather Conditions in Guangzhou City, China

Nan WANG*[1], Zhenhao LING[2], Xuejiao DENG[1], Tao DENG[1], Xiaopu LYU[3], Tingyuan LI[4], Xiaorong GAO[5], and Xi CHEN[6]

[1]*Institute of Tropical and Marine Meteorology, China Meteorological Administration, Guangzhou* 510000*, China*
[2]*School of Atmospheric Sciences, Sun Yat-sen University, Guangzhou* 510000*, China*
[3]*Department of Civil and Environmental Engineering, The Hong Kong Polytechnic University, Hong Kong* 999077*, China*
[4]*Ecological Meteorology Center, Guangdong Provincial Meteorological Bureau, Guangzhou* 510000*, China*
[5]*Guangzhou Meteorological Observatory, Guangzhou* 510000*, China*
[6]*School of Environmental Science and Engineering, Sun Yat-sen University, Guangzhou* 510000*, China*

(Received 29 August 2017; revised 28 December 2017; accepted 3 January 2018)

ABSTRACT

Historical haze episodes (2013–16) in Guangzhou were examined and classified according to synoptic weather systems. Four types of weather systems were found to be unfavorable, among which "foreside of a cold front" (FC) and "sea high pressure" (SP) were the most frequent (> 75% of the total). Targeted case studies were conducted based on an FC-affected event and an SP-affected event with the aim of understanding the characteristics of the contributions of source regions to fine particulate matter ($PM_{2.5}$) in Guangzhou. Four kinds of contributions—namely, emissions outside Guangdong Province (super-region), emissions from the Pearl River Delta region (PRD region), emissions from Guangzhou–Foshan–Shenzhen (GFS region), and emissions from Guangzhou (local)—were investigated using the Weather Research and Forecasting–Community Multiscale Air Quality model. The results showed that the source region contribution differed with different weather systems. SP was a stagnant weather condition, and the source region contribution ratio showed that the local region was a major contributor (37%), while the PRD region, GFS region and the super-region only contributed 8%, 2.8% and 7%, respectively, to $PM_{2.5}$ concentrations. By contrast, FC favored regional transport. The super-region became noticeable, contributing 34.8%, while the local region decreased to 12%. A simple method was proposed to quantify the relative impact of meteorology and emissions. Meteorology had a 35% impact, compared with an impact of −18% for emissions, when comparing the FC-affected event with that of the SP. The results from this study can provide guidance to policymakers for the implementation of effective control strategies.

Key words: WRF, Community Multiscale Air Quality model, source contribution, unfavorable weather system, fine particulate matter

Citation: Wang, N., Z. H. Ling, X. J. Deng, T. Deng, X. P. Lyu, T. Y. Li, X. R. Gao, and X. Chen, 2018: Source contributions to $PM_{2.5}$ under unfavorable weather conditions in Guangzhou City, China. *Adv. Atmos. Sci.*, **35**(9), 1145–1159, https://doi.org/10.1007/s00376-018-7212-9.

1. Introduction

Haze pollution, characterized by high levels of fine particles ($PM_{2.5}$—particles with a diameter less than 2.5 μm) and low visibility, is of increasing concern in China. Ambient particles can affect air quality and climate because they can absorb and scatter solar irradiation (Qiu et al., 1985; Watson, 2002; Hyslop, 2009; Cao et al., 2012). They also pose an adverse effect on human health. Studies have shown that high concentrations of $PM_{2.5}$ can increase morbidity and mortality, as well as affect the cardiovascular system (Dockery et al., 1993; Pope et al., 2009; Tie et al., 2009; IPCC, 2013).

Guangzhou is the capital of Guangdong Province and a megacity located in the city clusters of the Pearl River Delta (PRD) region (the PRD often refers to nine cities in Guangdong Province—namely, Guangzhou, Shenzhen, Dongguan, Foshan, Huizhou, Zhuhai, Zhongshan, Jiangmen, and Zhaoqing). With a population of more than 10 million, the city contributed 1.96×10^4 hundred million yuan to the GDP, ranking first in Guangdong Province, in 2016 (Guangdong Statistical Yearbook, 2016). However, rapid urbanization and economic growth have resulted in this city suffering from severe air pollution. In fact, Guangzhou has often been under low-visibility conditions since the 1980s (Deng et al., 2008).

* Corresponding author: Nan WANG
Email: wangn@grmc.gov.cn

During some extreme events, the daily average visibility can be less than 2 km, with the aerosol optical depth higher than 1.2 (Wu et al., 2005). High concentrations of $PM_{2.5}$ accompany these events (Zheng et al., 2011; Tao et al., 2012; Deng et al., 2014; Huang et al., 2014; Andersson et al., 2015; Mai et al., 2016). Facing enormous public pressure to ensure better air quality, the Chinese government has exerted considerable effort in mitigating air pollution. Each of its Five-Year Plans has set targets for primary emissions control, and volatile organic compound (VOC) emissions are going to be tightened, in addition to controlling emissions of sulfur dioxide (SO_2) and nitrogen oxides (NO_x) in the 13th Five-Year Plan (from 2016 to 2020). In 2013, the State Council released an "Air Pollution Action Plan", setting specific targets for developed areas, among which a 15% reduction goal was set for PRD $PM_{2.5}$ concentrations. In the local region, a series of emission control strategies have been implemented by the joint governments of Guangdong and Hong Kong. One example is the endorsed "PRD Air Pollutant Emission Reduction Plan Up to 2020". As a result, a declining trend of $PM_{2.5}$ in Guangzhou was measured between 2010 and 2015, with annual concentrations of 55, 41, 51, 53, 49 and 32 $\mu g\ m^{-3}$, respectively (Guangdong Year Book, 2010–15). Though the situation is becoming positive, there is still a long way to go, as the annual $PM_{2.5}$ concentration significantly exceeds the WHO guideline (annual mean of 10 $\mu g\ m^{-3}$). For policymakers, understanding source contributions to ambient $PM_{2.5}$ concentrations is the basis to further improve air quality in the PRD.

In recent years, a series of studies have been carried out to improve our knowledge of emissions and their contributions to ambient $PM_{2.5}$ in Guangzhou by using different methods—for instance, receptor models, tracing technology, and chemical transport models (CTMs) (Wang et al., 2005; Louie et al., 2005; Guo et al., 2009; Zhang et al., 2012; Gao et al., 2013). Xiao et al. (2011) used observations and Positive Matrix Factorization (PMF) to identify sources of submicron organic aerosols in a rural site of Guangzhou, reporting that primary organic aerosol constituted ~34–47% of organic aerosol, and secondary organic aerosol constituted ~53–66% of regional organic aerosol. Zheng et al. (2011) used the Chemical Mass Balance method to conduct source apportionment of carbonaceous aerosols in Guangzhou. It was found that primary emissions were important sources of excess organic carbon in the PRD. In addition, tracing technology, such as the use of isotopes, is also a good method. Liu et al. (2014) used radiocarbon (^{14}C) isotopes and tracers to conduct source apportionment of carbonaceous aerosols during winter in Guangzhou. Gao et al. (2012) combined PMF with tracer data and concluded that vehicular emissions, biomass burning and coal combustion were the main sources of polycyclic aromatic hydrocarbons in Guangzhou. Another mainstream method is the CTM. Wu et al. (2013) adopted CAMx-PSAT (Comprehensive Air Quality Model coupled with Particulate Source Apportionment Technology) in Hong Kong/the PRD and revealed that super-regional transport and mobile vehicles were the two major fine-particle sources in most cities of the PRD. Cui et al. (2015) claimed that stationary sources (industrial and power) made the largest contribution to $PM_{2.5}$ in Guangzhou, after conducting simulations with the Weather Research and Forecasting (WRF) Chemistry model. However, most previous studies were conducted to determine the possible contributions of individual sources, whereas few studies have focused on the impact of weather conditions on source contributions. In fact, the lifetime of $PM_{2.5}$ components and their precursors are different—both the generated $PM_{2.5}$ components and their precursors can be transported from region to region, depending on the synoptic weather conditions (Tan et al., 2009; Li et al., 2012; Liu et al., 2014). Furthermore, meteorological conditions also play important roles in the formation of secondary aerosols (Wang et al., 2009; Tan et al., 2013; Zhao et al., 2017). Therefore, to control $PM_{2.5}$ pollution in a specific location, in addition to identifying the impact of local sources, the impact of regional/super-regional sources, as well as meteorology, must be identified—especially under unfavorable weather conditions. Understanding to what degree ambient $PM_{2.5}$ originates from different sources under unfavorable weather conditions is critical for improving air quality in the PRD region. In the current work, source contribution studies were combined with synoptic meteorology. This combination can help to strengthen our knowledge of the characteristics of weather conditions during haze pollution, as well as help advance our knowledge of the contribution characteristics of a source region under a specific weather system. Since the prediction ability and forecast period of weather systems are currently relatively better and longer, respectively, than those of $PM_{2.5}$, the results from this study can provide guidance to policymakers so that targeted emissions control measures can be implemented in advance.

Historical haze episodes (2013–16) in Guangzhou were identified and classified according to weather systems. Case studies were performed by choosing two of the most unfavorable weather systems. We used the "brute-force method" with the aid of the WRF-CMAQ (CMAQ: Community Multiscale Air Quality) model to obtain the contributions of different sources to $PM_{2.5}$ in Guangzhou. Section 2 introduces the data used, the model system and the study method. Section 3 provides weather system analysis and observation analysis. Section 4 presents an evaluation of the modeling performance. The impact of source contributions and weather conditions are discussed in section 5. Finally, section 6 summarizes the results.

2. Model, data and methods

2.1. *Model system*

The CMAQ model, version 4.7.1 (http://cmascenter.org/cmaq/), was used to simulate $PM_{2.5}$ concentrations under two different typical meteorological conditions. Developed by the U.S. Environmental Protection Agency, CMAQ is a three-dimensional Eulerian CTM. It is designed for applications such as atmospheric air quality research and pol-

icy analysis and regulation. The WRF model, version 3.3.1 (http://www.wrf-model.org/index.php), was run to provide offline meteorological fields. The Meteorology Chemistry Interface Processor (version 3.6) was used to convert the WRF-produced meteorological data to the format required by CMAQ. Previous studies have shown that the WRF-CMAQ system is a powerful tool in simulating air quality, ranging from the city- to mesoscale level, in China (Wang et al., 2010; Che et al., 2011; Wang et al., 2015).

The WRF-CMAQ configurations were generally consistent with a previous study (Wang et al., 2016). In brief, a two-way nested domain was adopted with a grid resolution of 27 km and 9 km, with horizontal grids of 283×184 and 223×163, respectively. The outer domain covered the whole continental region of China, and the inner domain covered the entire region of Guangdong Province, with strong focus on the PRD region (see Fig. 1). The physical and chemical parameterization configurations were consistent with those presented in Wang et al. (2016).

We used the 2012-based Multi-resolution Emission Inventory for China (MEIC) to provide anthropogenic emissions for all selected scenarios. MEIC is a series of emission inventories for China and has a grid resolution of $0.25° \times 0.25°$ (He, 2012). It was developed by Tsing Hua University and considered five emission categories—namely, transportation, agriculture, power plants, industry and residence. In this study, MEIC was linearly interpolated to the model domain with consideration of Earth's curvature effect. For grids outside of China, the INDEX-B (Intercontinental Chemical Transport Experiment-Phase B) Asian emission inventory (Zhang et al., 2009) was used. The natural emissions for all scenarios were calculated offline using MEGAN (Model of Emissions of Gases and Aerosols from Nature), version 2.04 (Guenther et al., 2006).

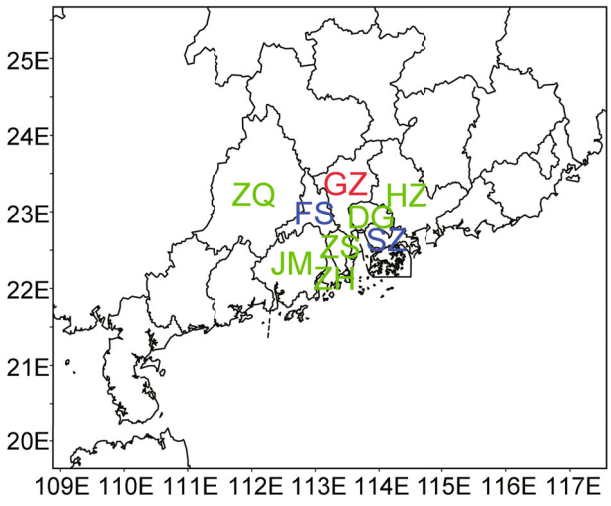

Fig. 1. Map of Guangdong Province, with nine cities(GZ, Guangzhou; FS, Foshan; SZ, Shenzhen; HZ, Huizhou; DG, Dongguan; ZQ, Zhaoqing; JM, Jiangmen; ZH, Zhuhai; ZS, Zhongshan) of the inner PRD highlighted.

2.2. *Unfavorable weather systems*

Studies have shown that air pollution in the PRD region is an integrated result of local (sources in the city areas), regional (other city sources within the region) and super-regional (all sources outside the study region) contributions (Kemball-Cook et al., 2009; Li et al., 2012). Understanding the specific contribution is fundamental for designing effective emission control strategies. One challenge is that the source contribution varies if weather conditions are different. In order to take the impact of weather into account, historical haze episodes from 2013 to 2016 were identified and classified according to weather systems. In this study, a haze episode was defined as a period with at least three consecutive haze days (a haze day refers to daily visibility less than 10 km and daily relative humidity (RH) less than 90%; rainy days are not considered). A similar method can be found in Wu et al. (2007). These data were collected from 86 operational automatic weather monitoring stations throughout Guangdong, and the data quality was well controlled by the China Meteorological Administration (CMA). Weather systems were classified by analyzing the weather charts of the selected haze episode. A similar method was used in previous studies (Chan and Chan, 2000; Huang et al., 2006; Saskia Buchholza et al., 2010; Li et al., 2011, 2016). According to this method, four types of weather systems—namely, "foreside of a cold front" (FC), "sea high pressure" (SP), "equalizing pressure" (EP) and "others" (Os, such as mainland high pressure and tropical cyclones)—were diagnosed as unfavorable weather systems in Guangdong Province (see Table 1). A general introduction to these weather systems is presented in the supplementary material (Fig. S1, see Electronic Supplementary Material), and more detailed information about the statistical data is given by Gao et al.[a]. On the one hand, the four-year statistical result showed that the haze episodes exhibited a declining trend. The total number of haze episodes from 2013 to 2016 was 61, 35, 30 and 19, respectively, which indicated that the emission control efforts were effective. The variation of annual concentrations of $PM_{2.5}$ also verified this positive aspect, with $PM_{2.5}$ concentrations of 53, 49, 32 and 30 $\mu g\ m^{-3}$, respectively. On the other hand, SP was the most frequent unfavorable weather system, accounting for 49.0% from 2013 to 2016. Among all the SP episodes, the lowest visibility (daily averaged) ranged from 0.7 km to 3.8 km, with the highest concentrations of $PM_{2.5}$ (daily averaged) ranging from 80 $\mu g\ m^{-3}$ to 184 $\mu g\ m^{-3}$, respectively. FC was the second most dominant unfavorable weather system, the occurrence of which comprised 26.9% of the total. Low visibility (0.6–5.4 km) and high $PM_{2.5}$ (79–222 $\mu g\ m^{-3}$) concentrations were also recorded. EP and Os were the last two, with occurrences of 16.6% and 7.6%, respectively. Since the total occurrence of haze episodes under SP and FC was over 75%, significantly higher than that under EP and Os ($p < 0.05$), targeted investigations were conducted by examining an SP-affected event (19–25 November 2014) and an FC-affected event (19–25 November 2010), with the aim of explaining the

[a]Gao et al., 2018: Characteristics and analysis on regional pollution process and circulation weather types over Guangdong Province, submitted.

Table 1. Information about haze episodes classified according to weather systems in Guangdong from 2013 to 2016.

	FC				SP			EP			Os			Total	
Year	No.	%	VIS	PM	No.	%	VIS	PM	No.	%	VIS	PM	No.	Annual Haze episodes	Annual $PM_{2.5}$ ($\mu g\ m^{-3}$)
2013	20	32.8%	0.6–4.7	–	28	45.9%	1.4–3.8	–	9	14.8%	1.4–2.8	–	4	6.6%	1.1–4.3	–	61	53
2014	11	31.4%	1.6–3.7	85–111	14	40.0%	1.1–3.4	88–142	7	20.0%	3.7–5.7	75–143	3	8.6%	1.5–7.3	86–128	35	49
2015	6	16.7%	1.9–4.3	79–222	19	60.0%	1.1–3.5	92–184	4	13.3%	3.5–9.3	75–103	3	10.0%	4.4–8.7	86–125	30	32
2016	3	15.8%	3.8–5.4	88–103	11	57.9%	0.7–3	80–179	4	21.1%	1.5–3.5	95–97	1	5.3%	2.6–8.9	87–97	19	30
all	39	26.9%	0.6–5.4	79–222	71	49.0%	0.7–3.8	80–184	24	16.6%	1.4–9.3	75–143	11	7.6%	1.1–8.9	86–128	145	–

Notes: No., number of haze episodes during the year; %, percentage of haze episodes during the year; VIS, range of lowest daily visibility among all the episodes collected in a weather system (units: km); PM, range of highest daily $PM_{2.5}$ concentration among all the episodes collected in a weather system (units: $\mu g\ m^{-3}$).

characteristics of source contributions under these two typical unfavorable weather systems.

2.3. *Scenario setting*

Figure 2 shows emissions categorized by administrative boundaries of provinces (Fig. 2a) and cities (Fig. 2b). It can be seen that emissions (SO_2, NO_x, Particulate matter between 2.5 and 10 μm (PMC), $PM_{2.5}$, carbon monoxide and VOCs) from Guangdong were the highest among the six provinces in southern China, with a total amount of 10.9×10^6 Mg yr^{-1} (unit area: 60.7 Mg yr^{-1} km^{-2}). Hunan ranked the second (total area: 9.9×10^6 Mg yr^{-1}; unit area: 46.7 Mg yr^{-1} km^{-2}), followed by comparative emissions from Guangxi (6.3×10^6 Mg yr^{-1}; unit area: 26.6 Mg yr^{-1} km^{-2}), Jiangxi (total area: 5.9×10^6 Mg yr^{-1}; unit area: 35.4 Mg yr^{-1} km^{-2}) and Fujian (4.1×10^6 Mg yr^{-1}; unit area: 33.1 Mg yr^{-1} km^{-2}). For cities within Guangdong Province, the inland nine PRD cities accounted for almost 70% of the emissions of the whole province. In particular, emissions from the GFS (Guangzhou, Foshan and Shenzhen) region were high: emissions from Guangzhou were the highest (total area: 1.7×10^6 Mg yr^{-1}; unit area: 0.23×10^3 Mg yr^{-1} km^{-2}), followed by Shenzhen (total area: 1.4×10^6 Mg yr^{-1}; unit area: 0.7×10^3 Mg yr^{-1} km^{-2}) and Foshan (total area: 1.2×10^6 Mg yr^{-1}; unit area: 0.31×10^3 Mg yr^{-1} km^{-2}). In fact, these three cities are topographically close to each other, so the contribution of GFS emissions is of interest in the following analysis.

Since the PRD is influenced by Asian monsoon circulations and the synoptic wind becomes a northerly wind in autumn and winter, the above emission patterns suggest that air quality in Guangzhou is likely to be influenced not only by local emissions but also emissions from nearby cities or provinces. With the objective of studying source contributions to Guangzhou, the term "local" in this paper indicates emissions from Guangzhou City (GZ), the term "region" refers to city sources within the PRD region, and the

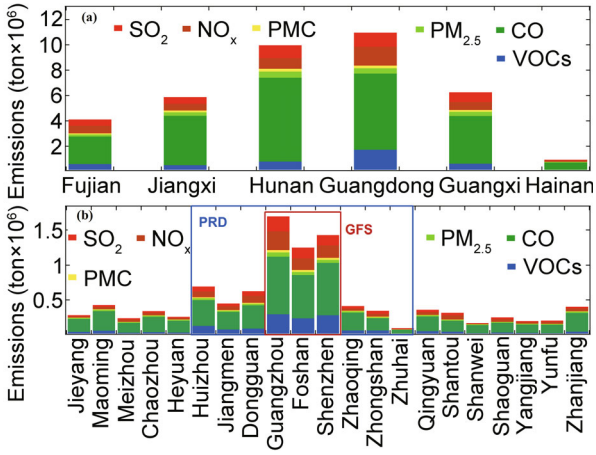

Fig. 2. Emissions categorized (a) by province in southern China and (b) by city in Guangdong Province. The blue frame highlights all cities of the inner PRD, and the red frame highlights three cities of the inner PRD—namely, Guangzhou, Foshan and Shenzhen.

term "super-region" implies contributions from sources (both anthropogenic and biogenic) outside Guangdong Province. One baseline emission scenario (BASE) and four emission reduction scenarios (ONLY_GD, NO_PRD, NO_GFS and NO_GZ) were used to study the possible source contributions under two unfavorable weather conditions (Table 2).

BASE refers to the scenario where $PM_{2.5}$ concentrations are simulated with the participation of the entire county-level emission inventories; the result represents the overall $PM_{2.5}$ contribution from all local and regional/super-regional sources without any reductions. ONLY_GD excludes all emissions except those from Guangdong, while NO_PRD, NO_GFS and NO_GZ pertain to emission inventories without emissions from the respective PRD region, GFS region, and GZ. By comparing the reduction scenarios with the baseline, contributions from different source regions could be identified. For example, the difference between ONLY_GD and BASE is the contribution from other provinces (super-regional contribution); similarly, the difference between NO_PRD and BASE, the difference between NO_GFS and BASE, and the difference between NO_GZ and BASE, are the contributions from the PRD region, the GFS region, and the local region, respectively. Hence, the difference (Δ) and source region contribution ratio (SRCR) are defined to quantify their specific contributions:

$$\Delta = \frac{\sum_{i=1}^{n_{\text{grid}}} (B_i - C_i)}{n_{\text{grid}}} \tag{1}$$

$$\text{SRCR} = \sum_{i=1}^{n_{\text{grid}}} \left(\frac{B_i - C_i}{B_i} \right) \times 100\% \tag{2}$$

where C is the $PM_{2.5}$ concentration simulated under an emission reduction scenario; B is the baseline $PM_{2.5}$ concentration; n_{grid} is the total grid number of Guangzhou coverage in the model domain; and B_i and C_i represent the $PM_{2.5}$ concentration within Guangzhou simulated under the baseline and an emission reduction scenario, respectively. To sum up, Δ (mass concentration variation) and SRCR (percentage variation) can reflect the impact of a source region on Guangzhou.

2.4. *Data used and model evaluation*

Hourly values of surface meteorological parameters such as temperature, wind, RH and pressure were adopted from the CMA. Meteorological data were collected at nine automatic weather stations in nine cities in the inland PRD region and used either for case analysis or for model validation. The air quality monitoring data used in this study were obtained from the Guangdong Province Environmental Administration (GDEPA) and the PRD Regional Air Quality Monitoring Network. The network consists of 16 sites, 13 of which lie within the inner PRD and three in Hong Kong. Previous studies have shown that these sites are well maintained and perform well in both scientific research and operational services (Zhong et al., 2013; Wang et al., 2016). In order to understand the two episodes controlled by unfavorable weather systems in Guangzhou, analyses of observed data were conducted to obtain the specific characteristics.

Statistical metrics, including mean values (Obs_{mean} and Sim_{mean}), mean bias (MB; MB = $\text{Obs}_{\text{mean}} - \text{Sim}_{\text{mean}}$), normalized mean bias (NMB;), root-mean-square error (RMSE;), and the index of agreement (IOA;), were used to assess the simulated results:

$$\text{NMB} = \sum_{i=1}^{n} \left[\frac{\text{Sim}(i) - \text{Obs}(i)}{\text{Obs}(i)} \right] \tag{3}$$

$$\text{RMSE} = \sqrt{\frac{1}{n} \sum_{i=1}^{n} (\text{Sim}(i) - \text{Obs}(i))^2} \tag{4}$$

$$\text{IOA} = 1 - \frac{\sum_{i=1}^{n} (\text{Sim}(i) - \text{Obs}(i))^2}{\sum_{i=1}^{n} (|\text{Sim}(i) - \overline{\text{Obs}}| + |\text{Obs}(i) - \overline{\text{Obs}}|)^2} \tag{5}$$

where n is the total number of samples, i indicates the ith sample, and Sim(i) and Obs(i) represent the ith simulated and observed values. Usually, a modeling result is acceptable if the NMB and RMSE values are close to 0 and the IOA value is close to 1 (Streets et al., 2007; Jiang et al., 2008, Xing et al., 2011; Wu et al., 2013; Wang et al., 2015, 2016).

3. Characteristics of observations

3.1. *Analysis of weather systems*

Figure 3 depicts the weather charts of a typical FC-affected event (2000 LST 21 November 2010) and a typical SP-affected event (0800 LST 20 November 2014). Usually, an FC-affected weather system occurs in a relatively cold season such as autumn, winter or early spring. On 19 Novem-

Table 2. Emission scenario setting for an FC-affected event and an SP-affected event.

Weather system	Case label	Emissions description	Purpose
S1: FC-affected event (19–25 November 2010)	BASE	Normal emissions	To compare with the other scenario
	ONLY_GD	Emissions only from Guangdong	To investigate the contribution from other provinces (super-regional contribution)
S2: SP-affected event (19–25 November 2014)	NO_PRD	Emissions except those from the PRD region	To investigate the contribution from the PRD region (PRD regional contribution)
	NO_GFS	Emissions except those from three major cities (GFS)	To investigate the contribution from the GFS region (GFS regional contribution)
	NO_GZ	Emissions except those from Guangzhou	To investigate the contribution from GZ (local contribution)

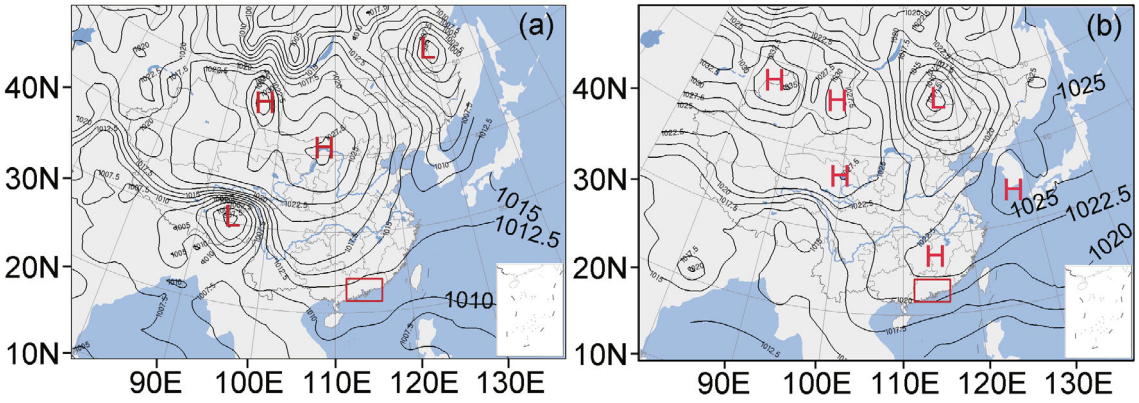

Fig. 3. Weather charts of (a) an FC-affected event at 2000 LST 21 November 2010 and (b) an SP-affected event at 0800 LST 20 November 2014. The red frame shows the PRD.

ber 2010, southern China experienced a mainland high (see Fig. S2), while a low-pressure system occurred over the Tibetan Plateau on 20 November, and this low pressure developed in an easterly direction (see Fig. S2). Then, the Tibetan low reached the mainland high on 21 November, and finally formed a cold front to the northwest of the PRD (Fig. 3a). Since the PRD was located on the foreside of this cold front, the weather conditions in the PRD were directly influenced. Usually, the northern parts of Guangdong experience a northerly cold wind, while the southern parts experience a southerly warm and humid air flow from the South China Sea. A convergence could elevate the warm and humid air flow, forming an inversion layer over the PRD region. Indeed, an inversion layer was observed during this FC-affected event, based on temperature sounding data at Qingyuan (in Guangzhou) and Kings Park (in Hong Kong) (see Fig. S3 in the supplementary material), confirming the accuracy of the weather system analysis. Under such a weather condition, air pollutants brought by the northerly wind from upwind areas could easily be trapped and accumulate in the PRD, thus causing air pollution.

An SP-affected weather system usually occurs in autumn, winter and spring. In most haze-related cases, the predecessor of a sea high is a mainland high (only a few are directly formed by a western Pacific subtropical high in summer). On 19 November 2014, a cold mainland high was moving easterly to the sea (Fig. S4); this cold high transformed once it encountered the warm marine atmosphere, and finally a slightly weaker but much warmer sea high was formed on 20 November (Fig. 3b). With the high-pressure center located over the sea, the ridge of this high extended southwesterly to the PRD and became the dominant weather system in the PRD. The PRD surface was dominated by downward anticyclonic air flows resulting in static wind on the ground (this was confirmed by the observed surface wind). Hence, such a weather condition would not be conducive to atmospheric dispersion and diffusion.

3.2. *Analysis of observations*

Figure 4 shows the patterns of wind, RH, pressure, temperature, $PM_{2.5}$ concentration and visibility during the FC-affected event. During this event, relatively strong northerly winds (daily mean wind speed = 2 m s^{-1}) were observed before the haze day (21 November), indicating the possible transport of air pollutants from Guangzhou to its downwind areas. In addition, a noticeable decreasing trend of diurnal pressure was observed compared to the relatively stable diurnal variations of RH and temperature. This was consistent with the weather system analysis in section 3.1, as the Tibetan low that reached southern China was conducive to regional transport. After the convergence of the northerly prevailing wind caused by the cold front and the southerly prevailing wind from the South China Sea (see discussion in section 3.1), haze days were observed on 21 November, 22 November, and 24 November, with the highest $PM_{2.5}$ concentrations of 110 μg m^{-3}, 102 μg m^{-3}, and 105 μg m^{-3}, and the lowest visibility of 0.9 km, 4 km and 2 km, respectively. Significant inverse relationships were observed between $PM_{2.5}$ concentration and visibility ($r = -0.61$) during these haze days. In addition, likely caused by the inversion layer, the wind pattern changed to weak southerly winds on the haze days (i.e., the daily mean wind speed on 21 November was only 1.0 m s^{-1}), suggesting the possible accumulation of air pollutants. Therefore, the relationship between the wind and $PM_{2.5}$ concentrations during this FC-affected event revealed that relatively strong northerly winds occurred before haze days (see 19 November and 21 November in Fig. 4), which may have played a role in reducing pollutant concentrations in Guangzhou, while the static southerly wind controlled the atmosphere on the haze days (see 21 November, 22 November and 24 November in Fig. 4), which might play a role in accumulating pollutants in Guangzhou.

The SP-affected event showed a different pattern (Fig. 5): there were three consecutive haze days starting from 20 November through 22 November, with the highest $PM_{2.5}$ concentration of 112 ug m^{-3} and the lowest visibility of 0.9 km during the haze episode. Though the wind directions varied considerably, the wind speed remained at rather low levels (mean wind speed = 0.9 m s^{-1}) during the haze event (20–22 November). The low wind speed indicated a stagnant atmospheric situation, since the PRD was fully controlled by SP. RH showed a stable variation, with a mean value of 68.5%,

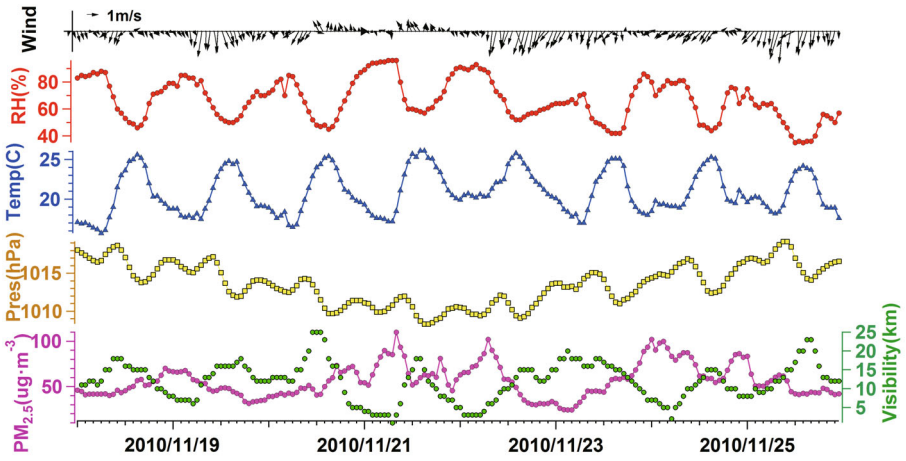

Fig. 4. Diurnal variation of surface wind, RH, pressure, temperature, $PM_{2.5}$ and visibility under the FC-affected weather system in November 2010.

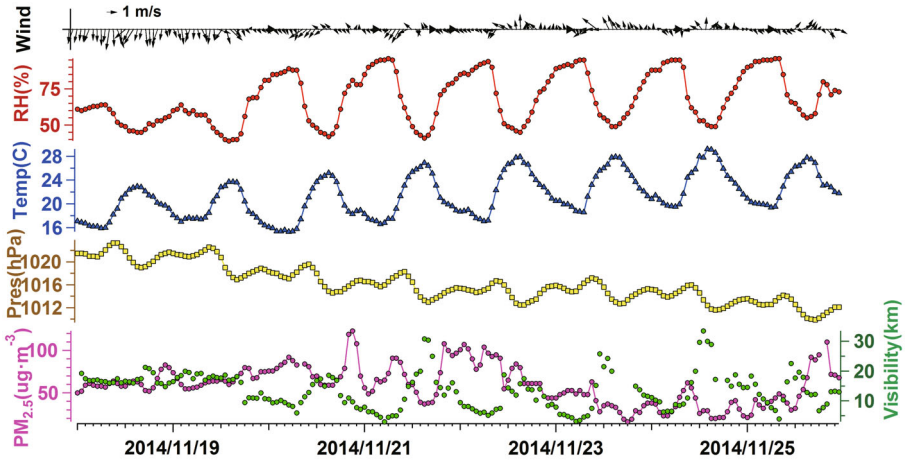

Fig. 5. Diurnal variation of surface wind, RH, pressure, temperature, $PM_{2.5}$ and visibility under the SP-affected weather system in November 2014.

indicating that the atmosphere was relatively dry. An increasing trend of temperature and a decreasing trend of pressure could be seen from 19 November to 20 November. This could be explained by the weather system evolution. The mainland cold high transformed when it encountered the warm marine atmosphere (see section 3.1). Though the pressure in the PRD decreased, the magnitude of the pressure under this SP-affected event remained high; the mean value during this episode was 1018 hPa—noticeably higher than that of the FC-affected event (1011 hPa). Therefore, the characteristic weather conditions under an SP-affected haze episode include a relatively high temperature, low humidity, static winds and high pressure. The atmosphere was not conducive to air pollutant dispersion, and local emissions appeared to be the dominant sources.

4. Evaluation of model performance

Given the analyses of weather systems in section 3.1 and the analyses of meteorological factors in section 3.2, it was found that the characteristics of the SP-affected event and the FC-affected event chosen in this study were consistent with the general overview (Li et al., 2016) about feature analysis of the typical FC weather system and SP weather system. Therefore, the two selected events could represent the general characteristics of SP and FC weather systems, respectively. Prior to using the modeling result to study the source contribution, an evaluation of model performance is necessary to verify the model simulation. The evaluation of the FC-affected event was presented previously (Wang et al., 2016), and the result showed that the simulation was well matched with the observation. Here, we present the evaluation of the SP-affected event.

Table 3 shows the average statistical comparisons between the simulated and observed values in this region. In general, the MB and NMB of temperature, RH and wind speed ranged between −1.9 and 1.2, and −0.01 and 1.3, respectively, showing the magnitudes matched well with the observations. The high values of IOA for temperature (0.9) and RH (0.8) also indicated a good agreement between the observed and simulated values. It was noted that the simulated wind speed values were generally overestimated, which

Table 3. Averaged model performance for temperature, RH, wind, $PM_{2.5}$ and O_3 during the SP-affected event (20–25 November 2014).

Simulated variable	Mean		MB	NMB	RMSE	IOA
	Obs	Sim				
T (°C)	22.5	21.3	1.2	−0.01	2.1	0.9
RH (%)	77.4	69.2	8.2	−0.1	10.7	0.8
WS (m s^{-1})	1.6	3.5	−1.9	1.3	2.2	0.4
$PM_{2.5}$ (μg m^{-3})	53.1	55.2	−2.1	0.2	29.6	0.5
O_3 (ppb)	31.4	44.3	−12.9	0.5	28.3	0.8

could have been due to the model resolution and the urban canopy structure. The grid resolution (9 km × 9 km) might be relatively too coarse to reveal the real geography, and the PBL scheme does not consider the urban canopy structure; therefore, uncertainties exist in wind calculations, as the distribution of urban morphology affects the surface-atmosphere energy budget (Jiang et al., 2008; Wang et al., 2015). Moreover, land surface modules, such as soil moisture, also result in uncertainty in the wind shear calculation (Li et al., 2013). Generally, the results were within the typical range of meteorological modeling studies (Chen et al., 2007; Wu et al., 2013; Cui et al., 2015; He et al., 2015; Wang et al., 2016).

The simulated $PM_{2.5}$ and ozone (O_3) concentrations were also evaluated. Three typical stations were selected as representatives (Huadu—a suburban site in northern Guangzhou; Panyu Middle School—an urban site in southern Guangzhou; and Xixiang—a coastal urban site in Shenzhen). Figure 6 shows that the time series of simulated $PM_{2.5}$ and O_3 values matched well with the observations. The simulated average $PM_{2.5}$ was 55.2 μg m^{-3}, which was close to the observed value (53.1 μg m^{-3}). Surface O_3 was slightly overestimated, with an MB of −12.9 ppb. The trends of the simulation were also comparable with those observed (IOA values were 0.5 and 0.8 for $PM_{2.5}$ and O_3, respectively). In addition, an area comparison was conducted for $PM_{2.5}$ evaluation. Observed $PM_{2.5}$ concentrations collected from GDEPA monitoring sites were interpolated throughout Guangdong (see Fig. 7a, which was downloaded from the Environmental Meteorology Operation-platform of Southern-China, EMOS, website: http://10.12.12.211/emos/index) and used to compare with simulations. It could be seen that high $PM_{2.5}$ concentrations were located in central Guangdong, i.e., the area where Guangzhou and Foshan are located; the concentrations were relatively well reproduced by the model. Overall, the spatial distributions showed that modelled $PM_{2.5}$ values agreed well with observations, indicating that the model also captured the regional pollution characteristics.

5. Source contributions

5.1. *Impact of local, regional and super-regional emissions*

The spatial impact of emissions from different source regions during the SP-affected event is shown in Fig. 8. Under such a stagnant weather condition, emissions outside Guangdong had limited influence on most cities throughout Guangdong. It could be seen that the main affected areas were those provincial boundaries where $PM_{2.5}$ concentrations decreased by 15–18 μg m^{-3}. However, a rather limited influence was observed in most PRD cities—for example, the $PM_{2.5}$ concentration in Guangzhou only decreased by 0–3 μg m^{-3}. Indeed, the average Δ between ONLY_GD and BASE was 2.3 μg m^{-3} in Guangzhou (Table 4). Compared to the influence of emissions outside Guangdong, emissions from the PRD region, GFS region and GZ mainly affected the $PM_{2.5}$ concentrations in areas within their specific administrative boundaries (Figs. 8b–d). Noticeable reductions in $PM_{2.5}$ were measured in Guangzhou; the Δ was 19.6 μg m^{-3}, 16.4 μg m^{-3} and 14.3 μg m^{-3} without the consideration of PRD regional emissions, GFS regional emissions and Guangzhou local emissions, respectively (Table 4). However, little influence could be found in areas outside these source regions. Such results suggested that the atmosphere was not favorable for regional transport, and local emissions became the dominant sources under the SP-affected weather conditions.

The spatial impact of super-regional, regional and local emissions indicated different patterns under the FC-affected event (Fig. 9). Emissions from outside Guangdong played a dominant role in contributing $PM_{2.5}$ to most areas of Guangdong. The area-mean $PM_{2.5}$ concentrations were reduced by 15.5 μg m^{-3} if these emissions were not considered. In fact, the average Δ between ONLY_GD and BASE was 14.3 μg m^{-3} (Table 4), which was significantly higher than that of the SP-affected event ($p < 0.05$), indicating that super-regional transport became an important contributor under the FC-affected weather system. With respect to the impact of regional emissions (NO_PRD minus BASE and NO_GFS minus BASE) and local emissions (NO_GZ minus BASE), the spatial differences in $PM_{2.5}$ concentrations displayed a "tongue-like" shape extending from the source regions to the southwest. The average Δ of the PRD region, the GFS region and local Guangzhou was 10.3 μg m^{-3}, 8.7 μg m^{-3}

Table 4. Statistics of $PM_{2.5}$ concentrations from different source regions during haze days in Guangzhou.

Parameter		Super-region		PRD region		GFS region		Local	
		SP	FC	SP	FC	SP	FC	SP	FC
Δ (μg m^{-3})	Max	0.1	0	1.8	0.2	1.5	0.2	1.4	0.2
	Min	4.7	56.1	38.6	37.0	32.2	27.3	30.2	22.2
	Average	2.3	14.3	19.6	10.3	16.4	8.7	14.3	7.6
SRCR		7.0%	34.8%	44.0%	16.0%	38.8%	13.6%	37.0%	12%

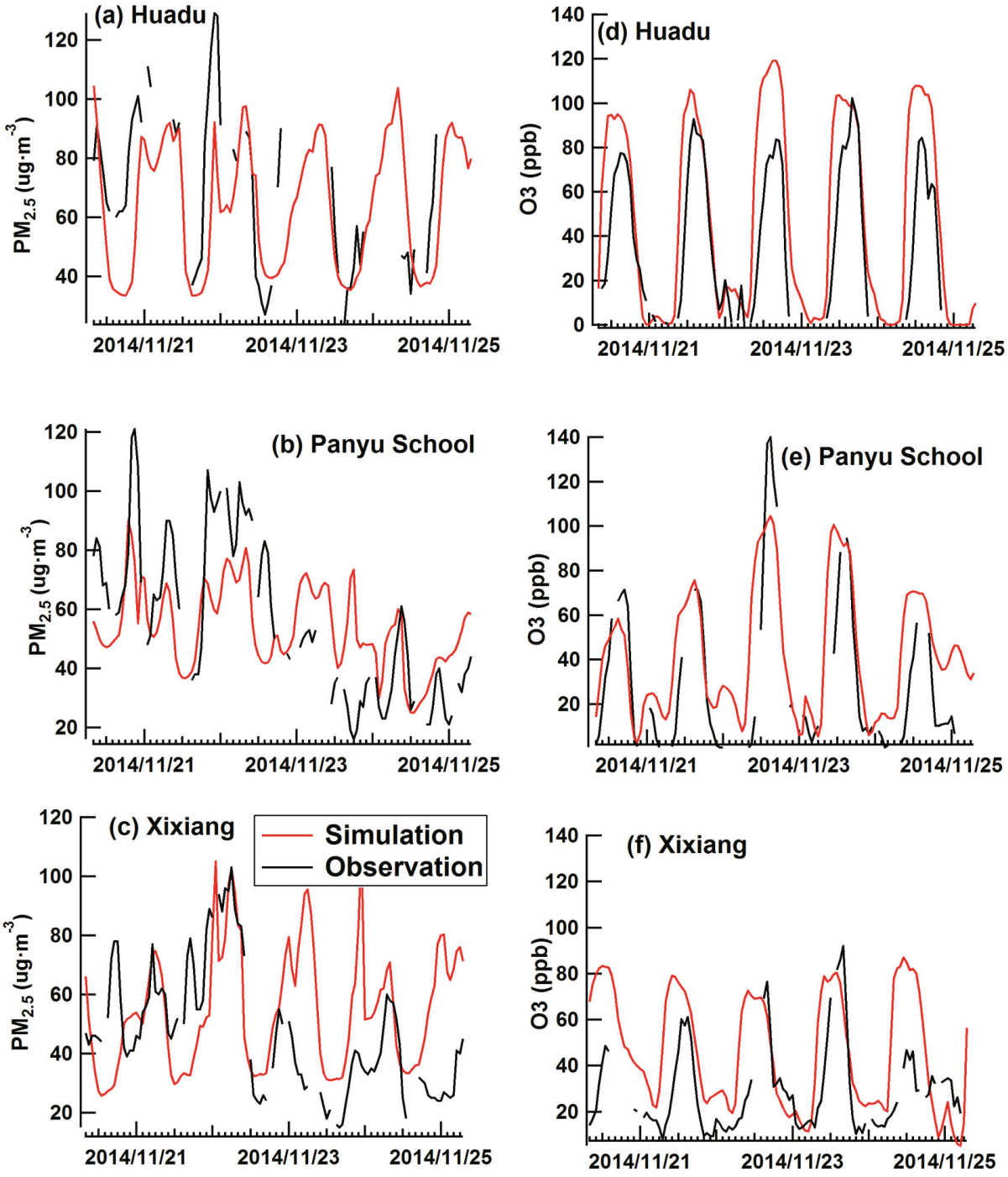

Fig. 6. Comparisons of simulated and observed $PM_{2.5}$ and O_3 at Huadu (a suburban site in northern Guangzhou), Panyu School (an urban site in southern Guangzhou) and Xixiang (a coastal urban site in Shenzhen) during the SP-affected event.

and 7.6 μg m^{-3}, with maximal reductions of 37 μg m^{-3}, 27.3 μg m^{-3} and 22.2 μg m^{-3}, respectively (see Table 4). It should be noted that these three source regions' contributions decreased, while the contributions from emissions outside Guangdong increased, compared to those under the SP-affected event. Such phenomena were consistent with the weather system analysis, i.e., the cold front resulted in a northerly wind in the PRD that transported air pollutants from source regions to downwind areas, thus resulting in the "tongue-like" shape. This finding also explained why super-regional transport became dominant under this condition, while the SP-affected event was a more stable condition since downward airflow dominated the atmosphere, trapping and accumulating emissions from source regions.

The contributions of specific source regions to $PM_{2.5}$ under these two typical unfavorable weather systems are

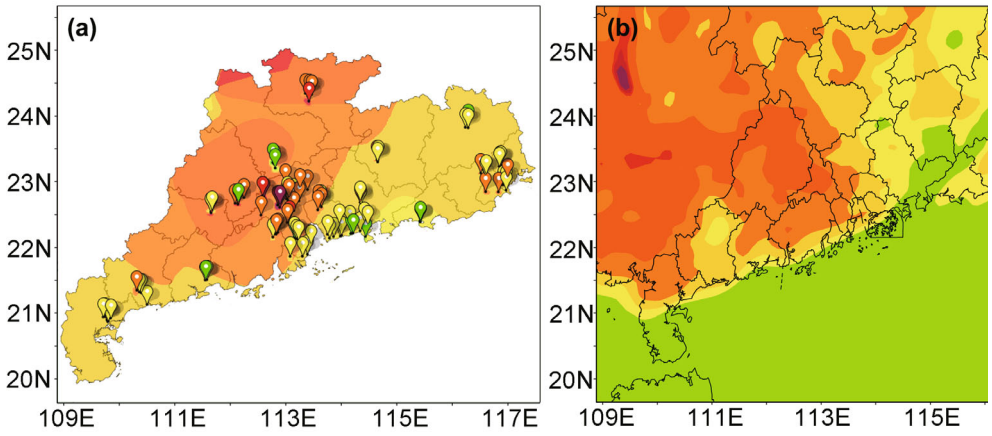

Fig. 7. Spatial comparison between observed $PM_{2.5}$ (units: ug m^{-3}) and simulated $PM_{2.5}$ over the PRD: (a) observed $PM_{2.5}$, in which the pins represent GDEPA monitoring stations and the contours were interpolated using monitoring values; (b) modelled $PM_{2.5}$, in which the bottom-right inset is a map of the South China Sea Islands.

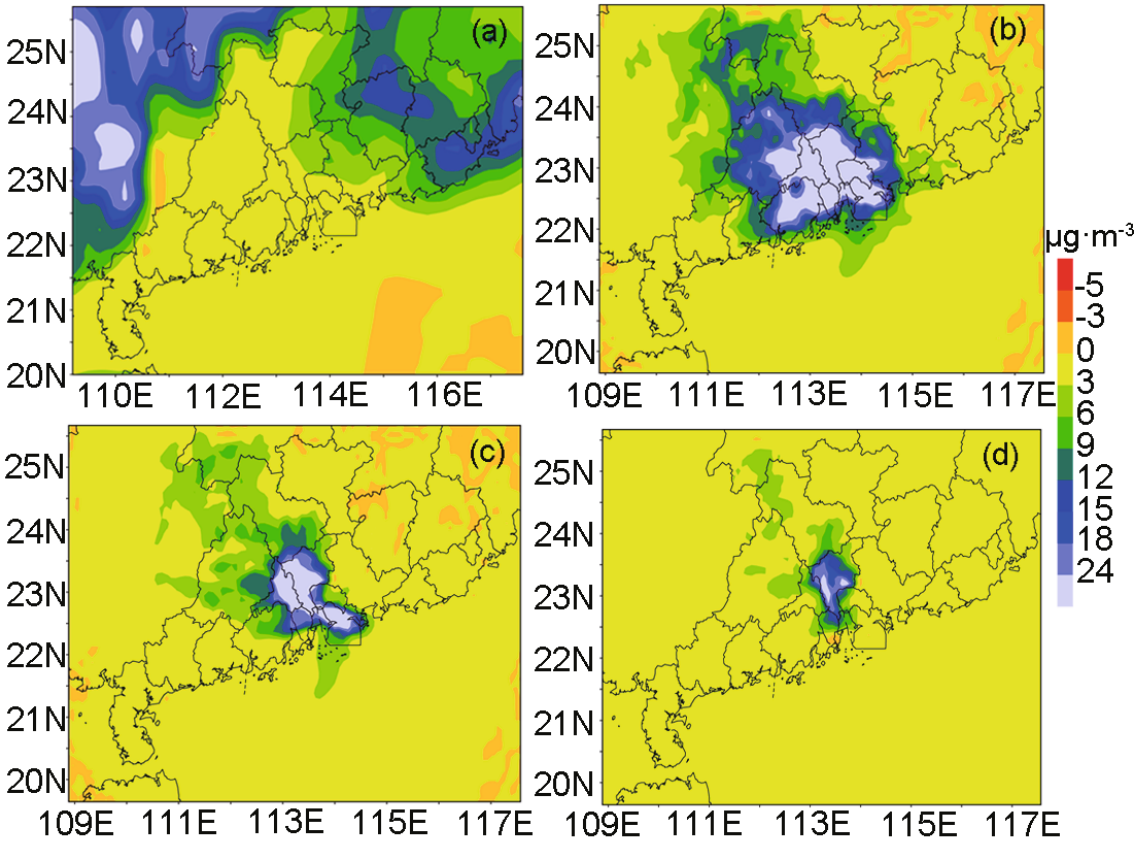

Fig. 8. Contributions from different source regions to 0800 LST average $PM_{2.5}$ during the haze days of the SP-affected event: (a) impact of emissions from outside Guangdong; (b) impact of emissions from the PRD; (c) impact of emissions from the GFS; (d) impact of emissions from Guangzhou.

presented in Fig. 10. When the sea high pressure system controlled weather conditions in the PRD, the SRCR of the PRD region ($SRCR_{PRD\ region}$), the SRCR of the GFS region ($SRCR_{GFS\ region}$) and the SRCR of Guangzhou ($SRCR_{Guangzhou}$) were 44.0%, 38.8% and 36.0%, respectively, which were all significantly higher than that of the super-region ($SRCR_{super\text{-}region}$; 7.0%). It should be noted that both the $SRCR_{PRD\ region}$ and the $SRCR_{GFS\ region}$ contained the source region contributions from Guangzhou; we used the difference between the regional values and the local values to deduct the contributions from Guangzhou. For example, the difference between $SRCR_{PRD\ region}$ and $SRCR_{Guangzhou}$ is the source contribution from the eight other inland PRD cities (excluding Guangzhou). It was found that the eight

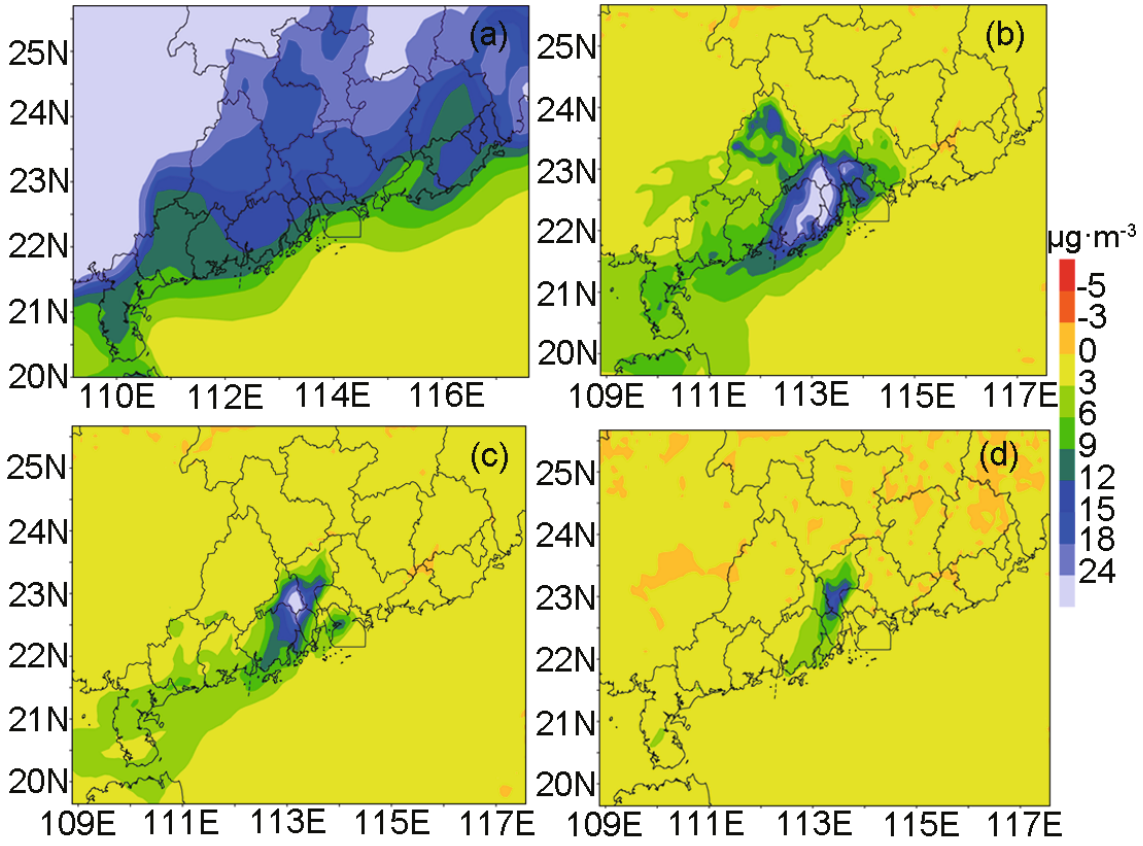

Fig. 9. Contributions from different source regions to 0800 LST average $PM_{2.5}$ during the haze days of the FC-affected event: (a) impact of emissions from outside Guangdong; (b) impact of emissions from the PRD; (c) impact of emissions from the GFS; (d) impact of emissions from Guangzhou.

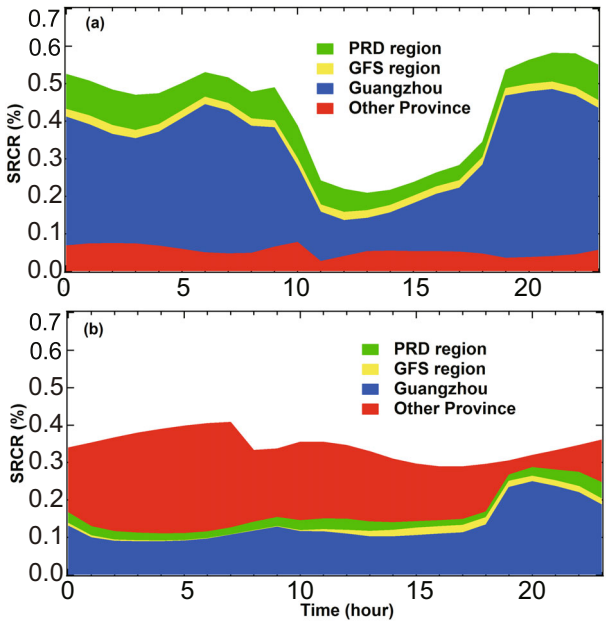

Fig. 10. $PM_{2.5}$ contributions from different source regions during the (a) SP- and (b) FC-affected events.

other inland PRD cities contributed 8%, whereas Foshan and Shenzhen contributed 2.8%. The results implied that local emissions were the major contributors to haze pollution, and it is strongly suggested that local emissions be reduced when formulating emission control strategies under a high-pressure system. With regard to the FC-affected event, the super-regional source became the dominant contributor (Fig. 10b) in Guangzhou. The $SRCR_{super\text{-}region}$ was 34.8%, which was significantly higher than that of the SP-affected event (SRCR = 7%; $p < 0.05$). In addition, the "tongue-like" shape in Fig. 9 indicated that regional transport should be noticeable, and the calculation of SRCR showed that regional source contributions were rather close to that of the local region ($SRCR_{PRD\ region}$, $SRCR_{GFS\ region}$ and $SRCR_{Guangzhou}$ were 16.0%, 13.6% and 12.0%, respectively). This is because Guangzhou is upwind in the PRD region, and the regional impact had greater influence in the downwind areas than in Guangzhou. Consequently, the super-regional contributions (emissions from the upwind area of Guangzhou) became dominant. Our results suggest that merely controlling local emissions under this weather condition is somewhat ineffective. By contrast, regional joint prevention and control should be considered to ensure a more reasonable control of haze pollution.

5.2. *Impact of weather conditions*

The above analysis demonstrates that source contributions to $PM_{2.5}$ in Guangzhou exhibit different characteristics under different weather systems. In fact, haze pollution is the

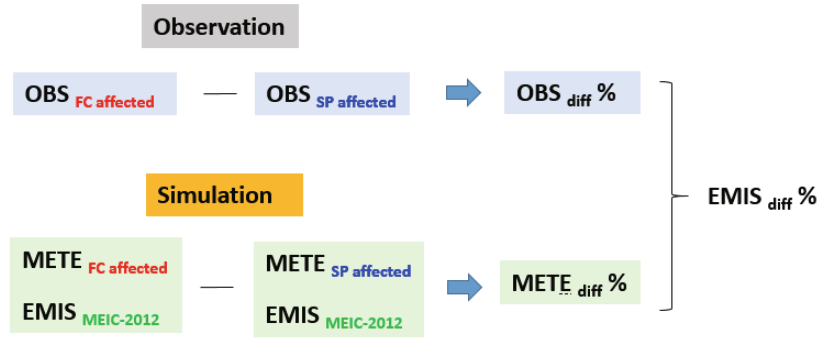

Fig. 11. A simple method to quantify the impact of meteorology and emissions.

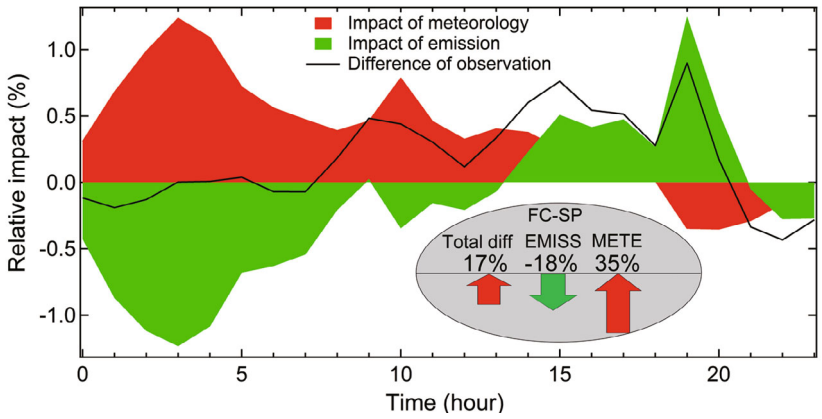

Fig. 12. Relative impact of meteorology and emissions between the FC- and SP-affected events.

integrated result of unfavorable weather conditions and emissions. In this section, we propose a simple method to distinguish the relative impact of meteorology and emissions.

Figure 11 presents the flowchart of this method. The observed difference (OBS_{diff}) can be directly calculated by comparing the observed $PM_{2.5}$ concentration of the SP-affected event and the FC-affected event. This OBS_{diff} can be regarded as the result of the difference between meteorology ($METE_{diff}$) and that of emissions ($EMIS_{diff}$) during two different periods. Then, $METE_{diff}$ can be obtained with the aid of a CTM. By using the same emissions ($EMIS_{2012\text{-}MEIC}$—the November emission inventory from 2012-MEIC) and different meteorologies ($METE_{FC\text{-}affected}$ and $METE_{SP\text{-}affected}$, produced by the WRF model) as input to drive the CMAQ model, the difference of the two simulations is $METE_{diff}$. Finally, $EMIS_{diff}$ can also be quantified after calculating OBS_{diff} and $METE_{diff}$. We know this method has uncertainties; the main uncertainty is introduced through the accuracy of model performance. For example, the emission inventory contains uncertainties itself; parameter schemes in numerical models can also bring uncertainties; and the overestimated surface wind may reduce air pollutant concentrations in upwind areas and increase the simulated results in downwind areas. However, since the simulated results have already passed strict evaluation, the results are considered acceptable. Furthermore, through the rapid development of numerical models, the uncertainty associated with the model has shown a decreasing trend. Therefore, this simple algorithm can be regarded as a means to quantify the relative impact of emissions and meteorology.

Figure 12 presents the relative impact of meteorology and emissions in two events, i.e., 35% and −18%, respectively. This result is consistent with the above analysis. On the one hand, the SP-affected event was a stagnant condition, and local emissions were the major contributors. On the other hand, super-regional transport was more important than local emissions for the FC-affected event. Therefore, the relative impact of meteorology was positive, while the impact of emissions was negative, when comparing the FC and SP-affected events.

6. Summary

In this study, source contribution studies were combined with synoptic meteorology to understand the contribution characteristics of source regions under different unfavorable weather systems.

Historical haze episodes (2013–16) in Guangzhou were examined and classified according to synoptic weather systems. Four types of weather systems were diagnosed as unfavorable: SP was ranked first (49.0%), followed by FC (26.9%), EP (16.6%) and Os (7.6%), in terms of the total number of haze events. Since the occurrence of FC and SP were the highest (> 75% of the total haze episodes), tar-

geted case studies were performed of an SP-affected event and an FC-affected event. Monitoring data showed that SP was characterized by low winds (0.9 m s^{-1}), relatively high pressure (1018 hPa) and low RH (68.5%). The high pressure-controlled system resulted in a rather stable atmosphere, and thus pollutants were trapped and not easily diffused. By contrast, FC was more favorable for pollutant transport. The cold front moved in a southeasterly direction, and synoptic winds prevailed in Guangdong. Northerly winds dominated and persisted at relatively high levels (2 m s^{-1}). Such a wind pattern was conducive to the transport of pollutants from upwind to downwind areas.

The numerical source regions' contribution results were consistent with the meteorological analysis. The source regions' contributions depicted different characteristics when different weather systems dominated. SP was a stagnant weather condition; the SRCR showed that the local region was a major contributor (37%), while the contributions of the PRD region (excluding Guangzhou), GFS region (excluding Guangzhou) and super-region were only 8%, 2.8% and 7%, respectively. By contrast, FC favored regional transport. The super-region became noticeable, contributing 34.8%, while the local region decreased to 12%. A simple method was proposed to quantify the relative impact of meteorology and emissions. The meteorological impact was 35%, while that of emissions was −18%, when comparing the FC-affected event with the SP-affected event.

Our results highlight the importance of the meteorological impact on the source region contribution. Attention should be paid to local emissions when an SP-type system dominates, while regional joint control should be initiated when an FC-type system is in control. This study can provide guidance to policymakers to implement effective control strategies under unfavorable weather systems.

Acknowledgements. This study was supported by the National Key R&D Program of China: Task 3 (Grant No. 2016 YFC0202000); Guangzhou Science and Technology Plan (Grant No. 201604020028); National Natural Science Foundation of China (Grant No. 41775037 and 41475105); Science and Technology Innovative Research Team Plan of Guangdong Meteorological Bureau (Grant No. 201704); Guangdong Natural Science Foundation-Major Research Training Project (2015A030308014); and a science and technology study project of Guangdong Meteorological Bureau (Grant No. 2015Q03). The author also thanks Tsinghua University for providing MEIC.

Electronic supplementary material Supplementary material is available in the online version of this article at https://doi.org/10.1007/s00376-018-7212-9.

REFERENCES

Andersson, A., J. J. Deng, K. Du, M. Zheng, C. Q. Yan, M. Sköld, and Ö. Gustafsson, 2015: Regionally-varying combustion sources of the January 2013 severe haze events over eastern China. *Environ. Sci. Technol*., **49**, 2038–2043, https://doi.org/10.1021/es503855e.

Cao, J. J., Q. Y. Wang, J. C. Chow, J. G. Watson, X. X. Tie, Z. X. Shen, P. Wang, and Z. S. An, 2012: Impacts of aerosol compositions on visibility impairment in Xi'an, China. *Atmos. Environ*., **59**, 559–566, https://doi.org/10.1016/j.atmosenv.2012.05.036.

Chan, C. Y., and L. Y., Chan, 2000: Effect of meteorology and air pollutant transport on ozone episodes at a subtropical coastal Asian city, Hong Kong. *J Geophys Res: Atmos* 105: 20707–24, https://doi.org/10.1029/2000JD900140.

Che, W. W., J. Y. Zheng, S. S. Wang, L. J. Zhong, and A. Lau, 2011: Assessment of motor vehicle emission control policies using Model-3/CMAQ model for the Pearl River Delta region, China. *Atmos. Environ*., **45**, 1740–1751, https://doi.org/10.1016/j.atmosenv.2010.12.050.

Chen, D. S., S. Y. Cheng, L. Liu, T. Chen, and X. R. Guo, 2007: An integrated MM5–CMAQ modeling approach for assessing trans-boundary PM_{10} contribution to the host city of 2008 Olympic summer games—Beijing, China. *Atmos. Environ*., **41**, 1237–1250, https://doi.org/10.1016/j.atmosenv.2006.09.045.

Cui, H. Y., W. H. Chen, W. Dai, H. Liu, X. M. Wang, and K. B. He, 2015: Source apportionment of $PM_{2.5}$ in Guangzhou combining observation data analysis and chemical transport model simulation. *Atmos. Environ*., **116**, 262–271, https://doi.org/10.1016/j.atmosenv.2015.06.054.

Deng, T., D. Wu, X. J. Deng, H. B. Tan, F. Li, and B. T. Liao, 2014: A vertical sounding of severe haze process in Guangzhou area. *Science China Earth Sciences*, **57**, 2650–2656, https://doi.org/10.1007/s11430-014-4928-y.

Deng, X.J, X. X. Tie, D. Wu, X. J., Zhou, X. Y. Bi, H. B. Tan et al., 2008: Long-term trend of visibility and its characterizations in the Pearl River Delta (PRD) region, China. *Atmospheric Environment*, 42 1424–1435, https://doi.org/10.1016/j.atmosenv.2007.11.025.

Dockery, D. W., and Coauthors, 1993: An association between air pollution and mortality in six U.S. cities. *New England Journal of Medicine*, **329**(24), 1753–1759, https://doi.org/10.1056/NEJM199312093292401.

Gao B., H. Guo, X.-M. Wang, X.-Y. Zhao, Z.-H. Ling, Z. Zhang, and T.-Y. Liu, 2012: Polycyclic aromatic hydrocarbons in $PM_{2.5}$ in Guangzhou, southern China: Spatiotemporal patterns and emission sources. *Journal of hazardous materials*, 239: 78–87, https://doi.org/10.1016/j.jhazmat.2012.07.068.

Gao, B., H. Guo, X. M. Wang, X. Y. Zhao, Z. H. Ling, Z. Zhang, and T. Y. Liu, 2013: Tracer-based source apportionment of polycyclic aromatic hydrocarbons in $PM_{2.5}$ in Guangzhou, southern China, using positive matrix factorization (PMF). *Environmental Science and Pollution Research*, **20**, 2398–2409, https://doi.org/10.1007/s11356-012-1129-0.

Guenther, A., T. Karl, P. Harley, C. Wiedinmyer, P. I. Palmer, and C. Geron, 2006: Estimates of global terrestrial isoprene emissions using MEGAN (model of emissions of gases and aerosols from nature). *Atmos. Chem. Phys.*, **6**, 3181–3210, https://doi.org/10.5194/acp-6-3181-2006.

Guo, H., A. J. Ding, K. L. So, G. Ayoko, Y. S. Li, and W. T. Hung, 2009: Receptor modeling of source apportionment of Hong Kong aerosols and the implication of urban and regional contribution. *Atmos. Environ*., **43**, 1159–1169, https://doi.org/10.1016/j.atmosenv.2008.04.046.

He, H., X. X. Tie, Q. Zhang, X. G. Liu, Q. Gao, X. Li, and Y. Gao, 2015: Analysis of the causes of heavy aerosol pollution in

Beijing, China: A case study with the WRF-Chem model. *Particuology*, **20**, 32–40, https://doi.org/10.1016/j.partic.2014.06.004.

He, K. B., 2012: Multi-resolution emission inventory for China (MEIC): model framework and 1990–2010 anthropogenic emissions. *Proceedings of International Global Atmospheric Chemistry Conference*, Beijing, China, AGU.

Huang, R. J., and Coauthors, 2014: High secondary aerosol contribution to particulate pollution during haze events in China. *Nature*, **514**, 218–222, https://doi.org/10.1038/nature13774.

Huang, J. P., J. C. H. Fung, and A. K. H. Lau 2006: Integrated processes analysis and systematic meteorological classification of ozone episodes in Hong Kong. *J. Geophys. Res*., 111, D20309, https://doi.org/10.1029/2005JD007012.

Hyslop, N. P., 2009: Impaired visibility: The air pollution people see. *Atmos. Environ*., **43**, 182–195, https://doi.org/10.1016/j.atmosenv.2008.09.067.

IPCC, 2013: *Climate Change 2013: The Physical Science Basis. Contribution of Working Group I Contribution to the Fifth Assessment Report of the International Panel on Climate Change*. Cambridge University Press.

Jiang, F., T. J. Wang, T. T. Wang, M. Xie, and H. Zhao, 2008: Numerical modeling of a continuous photochemical pollution episode in Hong Kong using WRF–chem. *Atmos. Environ*., **42**, 8717–8727, https://doi.org/10.1016/j.atmosenv.2008.08.034.

Kemball-Cook, S., D. Parrish, T. Ryerson, U. Nopmongcol, J. Johnson, E. Tai, and G. Yarwood, 2009: Contributions of regional transport and local sources to ozone exceedances in Houston and Dallas: Comparison of results from a photochemical grid model to aircraft and surface measurements. *J. Geophys. Res*., **114**, https://doi.org/10.1029/2008JD010248.

Li Y. M., X. J. Deng, T. Deng, Z. M. Lao, G. R. Xia. 2016: Haze characteristics associated with meteorological factors in Zhongshan during 2000~2014. *China Environmental Science*. **36**(6), 1638–1644. (in Chinese)

Li Y. M., S. J. Fan, R. W. Zhang. 2011: Study on air pollution meteorology over the Pearl River Delta during the autumn of 2008. *China Environmental Science*, **31**(10), 1585–1591. (in Chinese)

Li, Y., A. K. H. Lau, J. C. H. Fung, H. Ma, and Y. Tse, 2013: Systematic evaluation of ozone control policies using an Ozone Source Apportionment method. *Atmos. Environ*., **76**, 136–146, https://doi.org/10.1016/j.atmosenv.2013.02.033.

Li, Y., A. K. H. Lau, J. C. H. Fung, J. Y. Zheng, L. J. Zhong, and P. K. K. Louie, 2012: Ozone source apportionment (OSAT) to differentiate local regional and super-regional source contributions in the Pearl River Delta region, China. *J. Geophys. Res*., **117**, D15305, https://doi.org/10.1029/2011JD017340.

Liu, J. W., and Coauthors, 2014: Source apportionment using radiocarbon and organic tracers for $PM_{2.5}$ carbonaceous aerosols in Guangzhou, South China: Contrasting local- and regional-scale haze events. *Environ. Sci. Technol*., **48**, 12 002–12 011, https://doi.org/10.1021/es503102w.

Louie, P. K. K., J. C. Chow, L. W. A. Chen, J. G. Watson, G. Leung, and D. W. M. Sin, 2005: $PM_{2.5}$ chemical composition in Hong Kong: Urban and regional variations. *Science of the Total Environment*, **338**, 267–281, https://doi.org/10.1016/j.scitotenv.2004.07.021.

Mai, J. H., T. Deng, L. L. Yu, X. J. Deng, H. B. Tan, S. Q. Wang, and X. T. Liu, 2016: A modeling study of impact of emission control strategies on $PM_{2.5}$ reductions in Zhongshan, China, using WRF-CMAQ. *Advances in Meteorology*, **2016**, 5836070, https://doi.org/10.1155/2016/5836070.

Pope III, C. A., M. Ezzati, and D. W. Dockery, 2009: Fine-particulate air pollution and life expectancy in the United States. *New England Journal of Medicine*, **360**, 376–386, https://doi.org/10.1056/NEJMsa0805646.

Qiu, J. H., H. Q. Wang, X. J. Zhou, and D. R. Lu, 1985: Experimental study of remote sensing of atmospheric aerosol size distribution by combined solar extinction and forward scattering method. *Adv. Atmos. Sci*., **2**(3), 307–315, https://doi.org/10.1007/BF02677246.

Streets, D. G., and Coauthors, 2007: Air quality during the 2008 Beijing Olympic Games. *Atmos. Environ*., **41**, 480–492, https://doi.org/10.1016/j.atmosenv.2006.08.046.

Saskia Buchholza, Jürgen Junka, Andreas Krein et al, 2010: Air pollution characteristics associated with mesoscale atmospheric patterns in northwest continental Europe. *Atmospheric Environment*. 44 (2010) 5183-5190, https://doi.org/10.1016/j.atmosenv.2010.08.053.

Tan, J. H., J. C. Duan, K. B. He, Y. L. Ma, F. K. Duan, Y. Chen, and J. M. Fu, 2009: Chemical characteristics of $PM_{2.5}$ during a typical haze episode in Guangzhou. *Journal of Environmental Sciences*, **21**, 774–781, https://doi.org/10.1016/S1001-0742(08)62340-2.

Tan, H. B., Y. Yin, X. S. Gu, F. Li, P. W. Chan, H. B. Xu, X. J. Deng, and Q. L. Wan, 2013: An observational study of the hygroscopic properties of aerosols over the Pearl River Delta region. *Atmos. Environ*., **77**, 817–826, https://doi.org/10.1016/j.atmosenv.2013.05.049.

Tao, J., J. J. Cao, R. J. Zhang, L. H. Zhu, T. Zhang, S. Shi, and C. Y. Chan, 2012: Reconstructed light extinction coefficients using chemical compositions of $PM_{2.5}$ in winter in Urban Guangzhou, China. *Adv. Atmos. Sci*., **29**, 359–368, https://doi.org/10.1007/s00376-011-1045-0.

Tie, X. X., D. Wu, and G. Brasseur, 2009: Lung cancer mortality and exposure to atmospheric aerosol particles in Guangzhou, China. *Atmos. Environ*., **43**, 2375–2377, https://doi.org/10.1016/j.atmosenv.2009.01.036.

Wang, N., H. Guo, F. Jiang, Z. H. Ling, and T. Wang, 2015: Simulation of ozone formation at different elevations in mountainous area of Hong Kong using WRF-CMAQ model. *Science of the Total Environment*, **505**, 939–951, https://doi.org/10.1016/j.scitotenv.2014.10.070.

Wang, N. X. P. Lyu, X. J. Deng, H. Guo, T. Deng, Y. Li, C. Q. Yin, and S. Q. Wang, 2016: Assessment of regional air quality resulting from emission control in the Pearl River Delta region, southern China. *Science of the Total Environment*, **573**, 1554–1565, https://doi.org/10.1016/j.scitotenv.2016.09.013.

Wang, X. M., G. Carmichael, D. L. Chen, Y. H. Tang, and T. J. Wang, 2005: Impacts of different emission sources on air quality during March 2001 in the Pearl River Delta (PRD) region. *Atmos. Environ*., **39**, 5227–5241, https://doi.org/10.1016/j.atmosenv.2005.04.035.

Wang, X. M., F. Chen, Z. Y. Wu, M. G. Zhang, M. Tewari, A. Guenther, and C. Wiedinmyer, 2009: Impacts of weather conditions modified by urban expansion on surface ozone: Comparison between the Pearl River Delta and Yangtze River Delta regions. *Adv. Atmos. Sci*., **26**(5), 962–972, https://doi.org/10.1007/s00376-009-8001-2.

Wang, X. Y., and Coauthors, 2010: Process analysis and sensitivity study of regional ozone formation over the Pearl River Delta, China, during the PRIDE-PRD2004 campaign using the

Community Multiscale Air Quality modeling system. *Atmos. Chem. Phys.*, **10**, 4423–4437, https://doi.org/10.5194/acp-10-4423-2010.

Watson, J. G., 2002: Visibility: Science and regulation. *Journal of the Air & Waste Management Association*, **52**, 628–713, https://doi.org/10.1080/10473289.2002.10470813.

Wu, D. W., J. C. H. Fung, T. Yao, and A. K. H. Lau, 2013: A study of control policy in the Pearl River Delta region by using the particulate matter source apportionment method. *Atmos. Environ.*, **76**, 147–161, https://doi.org/10.1016/j.atmosenv.2012.11.069.

Wu, D., X. J. Deng, X. Y. Bi, F. Li, H. B. Tan, and G. L. Liao, 2007; Study on the visibility reduction caused by atmospheric haze in Guangzhou area. *Journal of Tropical Meteorology*, **13**, 77–80.

Wu, D., X. X. Tie, C. C. Li, Z. M. Ying, A. K. H. Lau, J. Huang, X. J. Deng, and X. Y. Bi, 2005: An extremely low visibility event over the Guangzhou region: A case study. *Atmos. Environ.*, **39**, 6568–6577, https://doi.org/10.1016/j.atmosenv.2005.07.061.

Xiao, R., and Coauthors, 2011: Characterization and source apportionment of submicron aerosol with aerosol mass spectrometer during the PRIDE-PRD 2006 campaign. *Atmos. Chem. Phys.*, **11**, 6911–6929, https://doi.org/10.5194/acp-11-6911-2011.

Xing, J., and Coauthors, 2011: Modeling study on the air quality impacts from emission reductions and atypical meteorological conditions during the 2008 Beijing Olympics. *Atmos. Environ.*, **45**, 1786–1798, https://doi.org/10.1016/j.atmosenv.2011.01.025.

Zhang, H. L., J. Y. Li, Q. Ying, J. Z. Yu, D. Wu, Y. Cheng, K. B. He, and J. K. Jaing, 2012: Source apportionment of $PM_{2.5}$ nitrate and sulfate in China using a source-oriented chemical transport model. *Atmos. Environ.*, **62**, 228–242, https://doi.org/10.1016/j.atmosenv.2012.08.014.

Zhang, Q., and Coauthors, 2009: Asian emissions in 2006 for the NASA INTEX-B mission. *Atmos. Chem. Phys.*, **9**, 5131–5153, https://doi.org/10.5194/acp-9-5131-2009.

Zhao, B., and Coauthors, 2017: Enhanced $PM_{2.5}$ pollution in China due to aerosol-cloud interactions. *Sci. Rep.*, **7**, 4453, https://doi.org/10.1038/s41598-017-04096-8.

Zheng, M., and Coauthors, 2011: Sources of excess urban carbonaceous aerosol in the Pearl River Delta Region, China. *Atmos. Environ.*, **45**, 1175–1182, https://doi.org/10.1016/j.atmosenv.2010.09.041.

Zhong, L.J., and Coauthors, 2013: The Pearl River Delta regional air quality monitoring network–regional collaborative efforts on joint air quality management. *Aerosol and Air Quality Research*, **13**, 1582–1597, https://doi.org/10.4209/aaqr.2012.L10.0276.